

## ORIGINAL RESEARCH ARTICLE

# Green synthesis of silver nanoparticles (CC-Ag NPs) utilizing the *cymbopogon citratus* extract and studying the antibacterial activity

Sahar A. Mamoori<sup>1</sup>, Ameer S. Muttaleb<sup>1</sup>, Issa Farhan D.<sup>2</sup>, Ehab K. Obaid<sup>1</sup>, Ali Jabbar Radhi<sup>3</sup>, Amjad Mirza Oda<sup>4,\*</sup>

<sup>1</sup> Department of Soil Science and Water Resource, College of Agriculture, Al-Qasim Green University, Al-Qasim District 964, Babylon 51013, Iraq

<sup>2</sup> Department of Optics Technologies, College of Health & Medical Techniques, Al-Mustaqlab University, Babylon, 6163, Iraq

<sup>3</sup> College of Pharmacy, University of Al-Kafeel, Najaf, 54001, Iraq

<sup>4</sup> Department of Science, College of Basic Education, University of Babylon, 51002, Iraq

\*Corresponding author: Amjad Mirza Oda, almajid1981@yahoo.com

## ABSTRACT

CC-Ag NPs (Silver nanoparticles) were synthesized from the leaf extract of *Cymbopogon citratus*. The biosynthesized silver nanoparticles were characterized by different analytical techniques. A characteristic absorption peak at 432 nm was observed which confirmed the surface plasmon resonance in silver nanoparticles (AgNPs). FTIR analysis showed the presence of bioactive compounds that take part in reduction and stabilization processes. The results of XRD analysis showed a crystalline phase formation only corresponding to silver nanoparticles. AFM and SEM analyses revealed that most of the particles are spherical with an average particle size of about 40 nm. The biosynthesized silver nanoparticles showed strong antibacterial effects against different pathogenic bacteria that covered both Gram-positive and Gram-negative strains. These included *Proteus mirabilis*, *Bacillus subtilis*, *Staphylococcus aureus*, *Escherichia coli*, *Klebsiella pneumoniae*, *Vibrio cholerae*, *Vibrio parahaemolyticus* and *Salmonella enteritidis*. Among all these tested organisms, the maximum zone of inhibition was observed against *Vibrio parahaemolyticus* with a diameter of 34.67mm. The concentration of the synthesized AgNPs solution used in these experiments was 1 mM.

**Keywords:** silver nanoparticles; antibacterial; *cymbopogon citratus*; AFM; XRD

## ARTICLE INFO

Received: 1 December 2025

Accepted: 20 January 2026

Available online: 26 January 2026

## COPYRIGHT

Copyright © 2026 by author(s).

*Applied Chemical Engineering* is published by Arts and Science Press Pte. Ltd. This work is licensed under the Creative Commons Attribution-NonCommercial 4.0 International License (CC BY 4.0).

<https://creativecommons.org/licenses/by/4.0/>

## 1. Introduction

Nanoparticles are the building blocks of nanotechnology. The particles have one or more dimensions of 100 nanometers or less. Nanoparticles exhibit different behavior from matter in its bulk scale. Various new applications are offered by nanotechnology in fields such as food processing, agriculture, and medicine<sup>[1-3]</sup>. Metal nanoparticles have been synthesized through various methods which include biological, physical and chemical approaches. The biological method has many advantages over the conventional chemical and physical techniques since it is cost-effective, fast and does not involve high pressure, high temperature, excessive energy or hazardous chemicals<sup>[4-6]</sup>. In biological synthesis, extracts are used as reducing and capping agents to produce (AgNPs), medicinal plants are mostly used for silver nanoparticle synthesis<sup>[7,8]</sup>. The reduction of metal ions contains phytochemicals in plant extracts comprising vitamins, enzymes, proteins, organic acids such as citrates and amino acids, and

polysaccharides that act as reducing and stabilizing agents capping agents. For instance, *Murraya koenigii* extract has been used for the green synthesis of silver nanoparticles mainly spherical-and cubic-shaped particles with an average size between 20-and 35 nm<sup>[9]</sup>. Seaweed-mediated silver nanoparticles have activity against the filariasis vector *Culex quinquefasciatus*<sup>[10]</sup>. *Sargassum muticum* mediated silver nanoparticles are crystalline; they are spherical in shape ranging from 43-79 nm<sup>[11]</sup>.

*Cymbopogon* is a genus belonging to about 55 species widely known as tropical/subtropical lemon grasses under family Gramineae (Poaceae). It is one amongst best known aromatic weeds because of its high content essential oil. *Cymbopogon* is cultivated over large areas in the tropical and subtropical regions of Africa, America and Asia. *Cymbopogon citratus* has had traditional uses in different countries as herbal tea, pharmaceutical supplements, insect repellent and insecticide, anti-inflammatory and analgesic applications. In Nigeria, the tummy disorders and malaria treatment comprise its traditional use besides an antioxidant application. The essential oil of *Cymbopogon citratus* always contains bioactive components comprising hydrocarbon terpenes, alcohols, ketones, esters, and mainly aldehydes such as citral<sup>[12-15]</sup>. The silver nanoparticles have antibacterial activity dependent on their size; smaller particles have enhanced bactericidal effects due to a larger surface area-to-volume ratio. Therefore, smaller silver nanoparticles present more surface area for contact with microbial cells which results in more effective antimicrobial activity than larger ones<sup>[16-18]</sup>.

## 2. Material and Methods

### 2.1. Synthesis of silver nanoparticles

Fresh leaves of *Cymbopogon citratus* were collected from local farms in Babylon. The leaves were washed thoroughly with distilled water three times to remove surface contaminants and then cut into small pieces. Approximately Ten grams of this material was mixed with 60 mL of distilled water and the mixture was allowed to boil at 80 °C for fifteen minutes. It was then brought down to room temperature before filtering through Whatman No.1 filter paper so as to get clear plant extract. To synthesize silver nanoparticles, 20 mL of *C. citratus* extract was added to 180 mL of 1 mM silver nitrate (AgNO<sub>3</sub>) solution purchased from BDH Chemicals, U.K. The mixture was subjected to heating at a temperature of 80 °C for 15 minutes. A distinct change in color from pale yellow to brown proves successful formation of silver nanoparticles hence reduction of Ag<sup>+</sup> to Ag<sup>0</sup>.

### 2.2. Characterization of the synthesized silver nanoparticles

A UV-Visible spectrophotometer (LF 4030, Scienco, Korea) was used to determine the optical properties of silver nanoparticles. The absorption spectra were recorded within a range from 200 nm to 800 nm. An Atomic Force Microscope (AFM) (AA 3000, Angstrom Advanced Inc.) was employed for surface morphological studies of synthesized nanoparticles. Dynamic Light Scattering (DLS) analysis by a SALD-210 particle size analyzer determined the particle size distribution in the sample. Fourier transform infrared spectroscopy (FTIR) (IR Affinity, Shimadzu) analyzed and detected functional groups found on AgNPs surfaces. X-ray Diffraction (XRD) analysis identified crystalline phases present inside synthesized nanoparticles carried out at Cu K $\alpha$ 1 radiation  $\lambda=1.540562\text{\AA}$ ; current =30mA; voltage =40kV (DX -2700 SSC, USA). Morphology and surface characteristics have been further examined by Scanning Electron Microscopy (SEM) on an Inspect 550 instrument, Netherlands, at 25 kV accelerating voltage. The stability of the green synthesized silver nanoparticles has been checked for a period of one month by UV–Vis spectroscopy.

### 2.3. Antibacterial activity of silver nanoparticles

Antibacterial activities of synthesized silver nanoparticles were tested against eight strains of bacteria which included *Proteus mirabilis*, *Bacillus subtilis*, *Staphylococcus aureus*, *Escherichia coli*, *Klebsiella*

*pneumoniae*, *Vibrio cholerae*, *Vibrio parahaemolyticus* and *Salmonella enteritidis* by the agar well diffusion method<sup>[19]</sup>. All the bacterial strains were grown on Mueller-Hinton agar. Agar plates were prepared and wells of 6 mm diameter made using a sterile gel borer. 50  $\mu$ L solution of silver nanoparticles was added into each well. Control wells containing sterile distilled water (negative control), plant extract alone, and silver nitrate solution alone were also included on each plate. Additionally, a positive control using a standard antibiotic disc (e.g., ampicillin) was included for comparison. The plates were incubated at 37 °C for 24 hr. After incubation, the diameters (in mm) zones of inhibition were measured to check antimicrobial activity of nanoparticles.

### 3. Result and Discussion

#### 3.1. Characterization of the synthesized silver nanoparticles

The formation of silver nanoparticles (AgNPs) was first indicated by a visible color change due to the reduction of silver ions ( $\text{Ag}^+$ ) to elemental silver ( $\text{Ag}^0$ ). This bioreduction is facilitated by several bioactive compounds present in *Cymbopogon citratus* leaf extract comprising vitamins, polyphenols, tannins, and other phytochemicals that act as natural reducing and stabilizing agents<sup>[4,5,20]</sup>. **Figure 1** shows UV-Visible absorption spectra for synthesized silver nanoparticles. The surface plasmon resonance (SPR) band of CC-Ag NPs (AgNPs) synthesized using *C. citratus* extract has been observed within the range between 350 nm and 550 nm with maximum absorption peak ( $\lambda_{\text{max}}$ ) at 432 nm. A sharp peak is observed due to the excitation of SPR which is defined as a collective oscillation mode of conduction band electrons at the nanoparticle surface in phase with the incident light wave<sup>[21]</sup>. The conduction and valence bands in silver are very close to each other, permitting free movement of electrons. This enhances strong absorption within the visible region characteristic features for AgNPs.

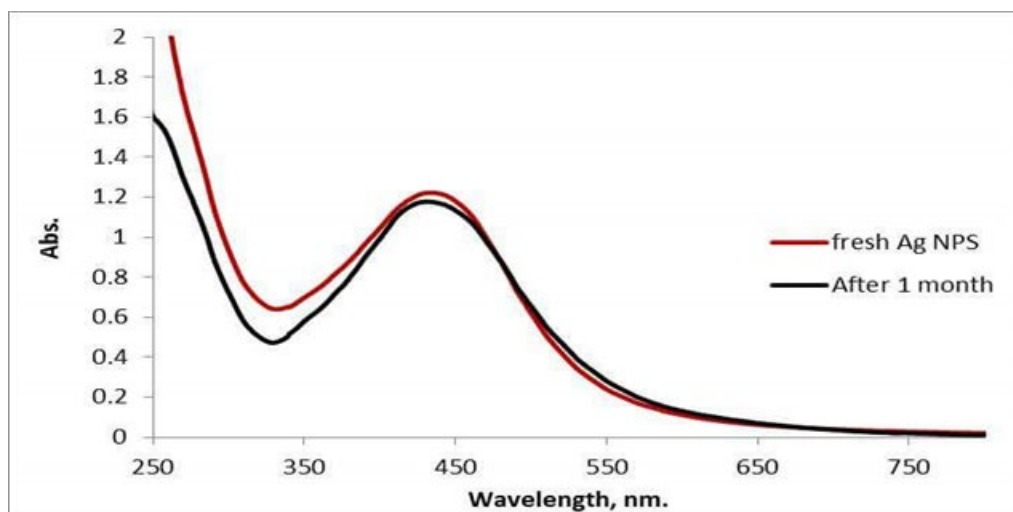


**Figure 1.** UV-Visible absorption spectra of silver nanoparticles synthesized using *Cymbopogon citratus* leaf extract. The red line represents the freshly prepared AgNPs solution, while the black line corresponds to the same solution after one month of storage. A distinct surface plasmon resonance (SPR) peak is observed around 432 nm, indicating the formation and stability of the nanoparticles over time.

Surface plasmon resonance (SPR) bands appear in silver nanoparticles (AgNPs). They vary with the size and anisotropy of shape of the particles. A small, nearly spherical AgNPs will have a narrow symmetric SPR band which gives a single peak in the absorption spectrum. Larger particles having different shapes or sizes possess broader SPR bands and may show two or more distinct peaks in the spectrum<sup>[22]</sup>. As seen in **Figure 1**, a symmetric SPR band is centered at 432 nm (the red line) which shows there is a narrow size distribution and perfectly spherical morphology of the freshly prepared AgNPs. The black line shows the SPR band of similar AgNPs stored for about one month. Therefore, this kind of similarity between the absorption spectra both from

fresh and stored nanoparticles with specific reference to an unaltered SPR peak position minimal change in absorbance no broadening of the band signifies that they are stable over one month<sup>[21]</sup>.

Fourier Transform Infrared (FTIR) spectroscopy analysis was carried out on **CC-Ag NPs** (AgNPs) synthesized using *Cymbopogon citratus* (lemongrass) leaf extract so as to determine surface functional groups see **Figure 2**; hence active phytochemical components adsorbed onto nanoparticle surface during synthesis will be detected by this analysis too! A strong band observed around  $3375.43\text{ cm}^{-1}$  is assigned to O-H stretching vibrations. A peak around  $3294.92\text{ cm}^{-1}$  corresponds to N-H stretching  $\text{NH}_2$  groups, indicative of the reducing ability of *C. citratus* extract. A band at  $2983.8\text{ cm}^{-1}$  is assigned to C-H stretching vibrations. The peak at  $1749\text{ cm}^{-1}$  is associated with C=O stretching, thereby suggesting the presence of either aldehydes or ketones or carboxylic acids. The band at  $1637\text{ cm}^{-1}$  also relates to amine  $\text{NH}_2$  functional group. Bands found further low include a band at  $1110\text{ cm}^{-1}$  (O-H bending vibrations), a band  $1080\text{ cm}^{-1}$  (attributed to C-O stretching) and a band  $823\text{ cm}^{-1}$  (associated with C-H deformation). These functional groups show the presence of phytochemicals adsorbed onto the surface of AgNPs. This organic layer is both reducing and stabilizing (capping) agent which forms a protective shell around the nanoparticles. Therefore, *C. citratus* extract reduces silver ions to facilitate the reduction but also contributes towards stabilization of the nanoparticles<sup>[22-25]</sup>.

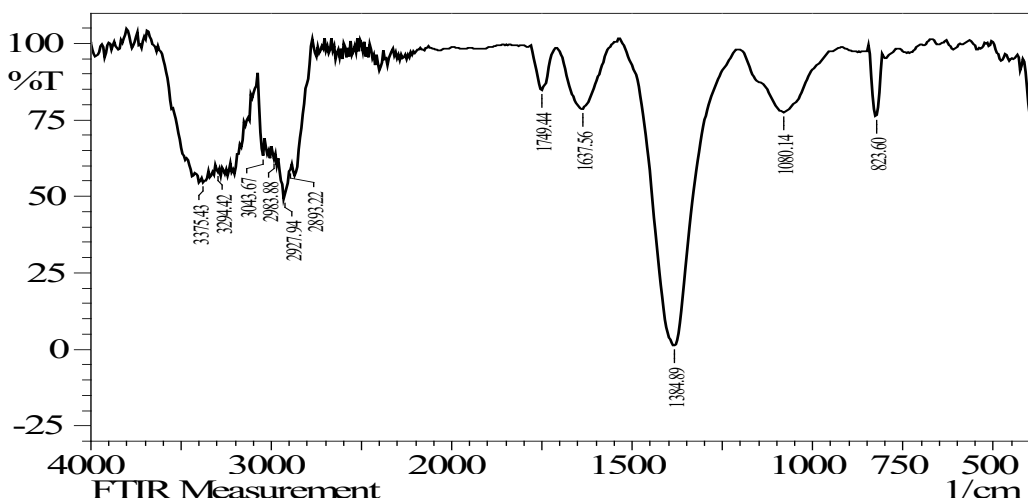


**Figure 2.** FTIR spectrum of silver nanoparticles synthesized using *Cymbopogon citratus* (lemongrass) leaf extract, showing the functional groups responsible for reduction and stabilization of AgNPs.

The crystalline nature of silver nanoparticles synthesized using *Cymbopogon citratus* leaf extract is evident from the results of X-ray diffraction analysis illustrated in **Figure 3**. The XRD pattern was recorded within a  $2\theta$  range between  $20^\circ$  and  $60^\circ$ , with very intense diffraction peaks observed at  $38.68^\circ$  and  $44.29^\circ$  corresponding to (111) and (200) planes of FCC structure respectively, (JCPDS file no.:04-0783). These results show the successful formation of pure crystalline AgNPs. There are no detectable peaks corresponding to any silver oxide phases. The biosynthesis process has completely reduced silver ions to metallic silver nanoparticles by using *C. citratus* extract. The broadened diffraction peaks give an idea about the particle size of synthesized AgNPs. The average crystallite size (D) was calculated by using The Debye–Scherrer equation (1).

$$D = \frac{0.94\lambda}{B \cos\theta} \quad (1)$$

where:

D is the crystallite size,

$\lambda = 1.54060\text{ \AA}$  (Cu K $\alpha$  radiation),

$\theta$  is the Bragg diffraction angle,

$B$  is the full width at half maximum (FWHM) of the peak in radians,

0.94 is the shape factor constant.

Based on this calculation, the average crystallite size of the biosynthesized AgNPs was estimated to be approximately 28 nm, further confirming the formation of nanoscale materials<sup>[24-26]</sup>. This result (28 nm from XRD) is smaller than the average size obtained from AFM (40 nm) and significantly smaller than the DLS result (174 nm). These differences are expected due to the fundamental measurement principles of each technique, as discussed later in the DLS section.

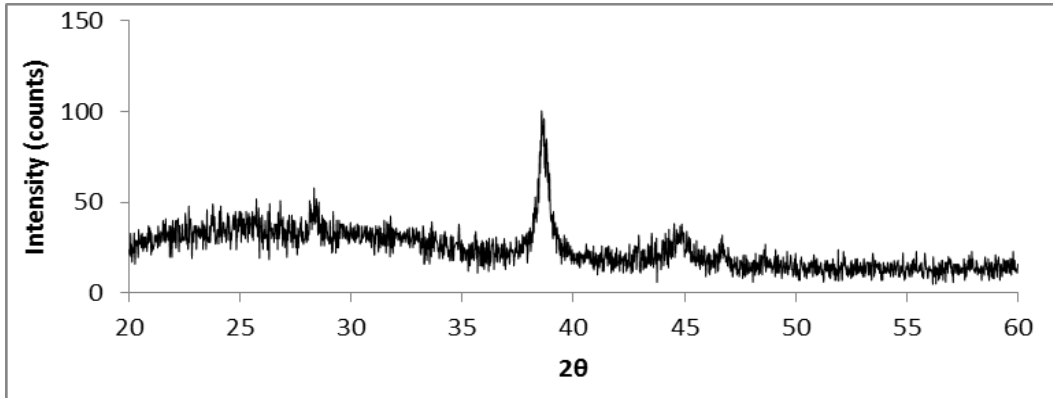


**Figure 3.** XRD pattern of silver nanoparticles synthesized using *Cymbopogon citratus* leaf extract, showing characteristic peaks for face-centered cubic (FCC) silver and confirming the crystalline nature of the nanoparticles.

**Figure 4** shows an Atomic Force Microscopy (AFM) image displaying the surface topography of silver nanoparticles synthesized by using the leaf extract of *Cymbopogon citratus*. The average particle size of synthesized AgNPs was about 40 nm. A three-dimensional AFM image, as seen in **Figure 4(a)**, describes compact nanoparticles with relatively high surface roughness values. The minimum and maximum particle sizes were found to be 10 nm and 120 nm, respectively, most probably at about 25 nm as shown by granularity normal distribution depicted in **Figure 4(b)**.

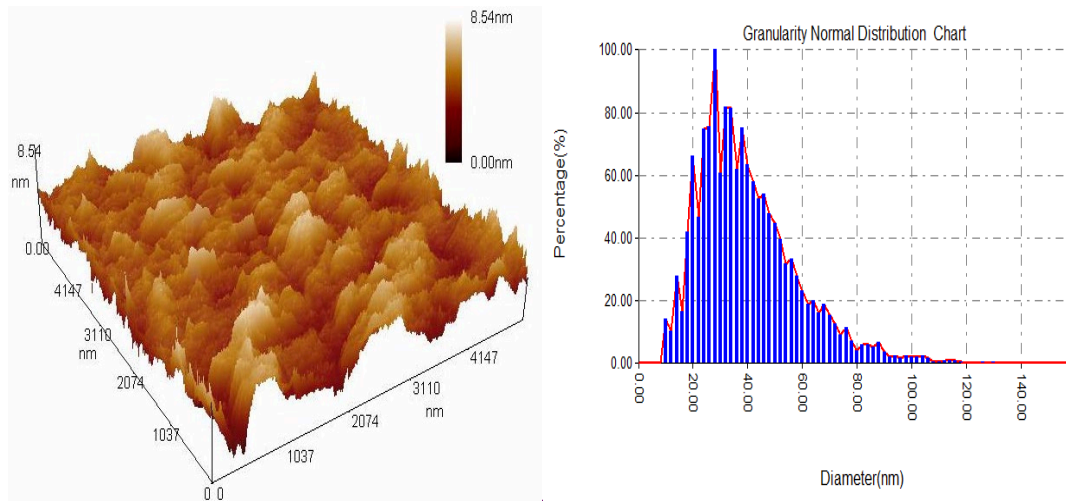


**Figure 4. (a)** Three-dimensional AFM image of silver nanoparticles synthesized using *Cymbopogon citratus* leaf extract, illustrating surface morphology and topography; (b) Granularity normal distribution showing particle size distribution of the AgNPs.

Dynamic light scattering (DLS) was used to study the particle size distribution of silver nanoparticles and also to make a comparison between these sizes and those obtained by other techniques. DLS measures

hydrodynamic diameter, which includes the core nanoparticle and any molecules attached to its surface. As evident from **Figure 5**, results of DLS revealed an average particle size of 174 nm with a size distribution range between about 80-200 nm. This is much larger than average sizes reported from scanning electron microscopy (SEM) and atomic force microscopy (AFM). The difference observed emanates from basic differences in measurement principles. SEM and AFM determine physical core sizes of nanoparticles without considering any adsorbed surface layers while DLS measures hydrodynamic diameter that includes not only the core particle but also a surrounding shell formed by ions/molecules/phytochemical capping agents attached on the surface<sup>[27]</sup>. The DLS results suggest a tendency for the nanoparticles to agglomerate in the aqueous solution.

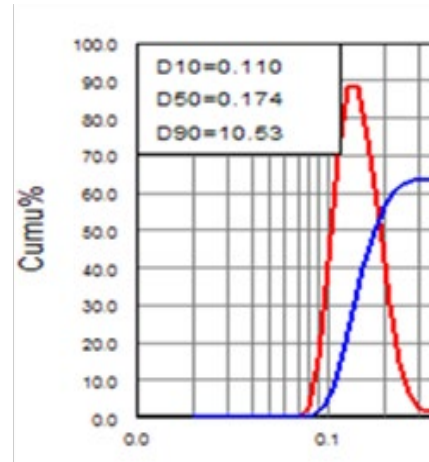


**Figure 5.** Particle size distribution of silver nanoparticles synthesized using *Cymbopogon citratus* leaf extract, as determined by dynamic light scattering (DLS).

Morphology and nanostructure characterization of silver nanoparticles (AgNPs) were carried out by scanning electron microscopy (SEM). SEM micrographs of AgNPs synthesized using *Cymbopogon citratus* leaf extract are presented in **Figure 6**. The images show mostly spherical nanoparticles which agglomerate on the removal of solvent. A low magnification image (left) shows a rough surface texture with uniformly shaped particles having narrow size distribution and displaying little agglomeration. A higher magnification image, 400nm scale shows fine spherical particles whose average particle size ranges between 30 to 80 nm. These results show that green synthesis adequately prepares silver nanoparticles of regular morphology and appropriate nanoscale dimensions through *C. citratus* leaf extract, hence its potential application for nanomaterial fabrication.

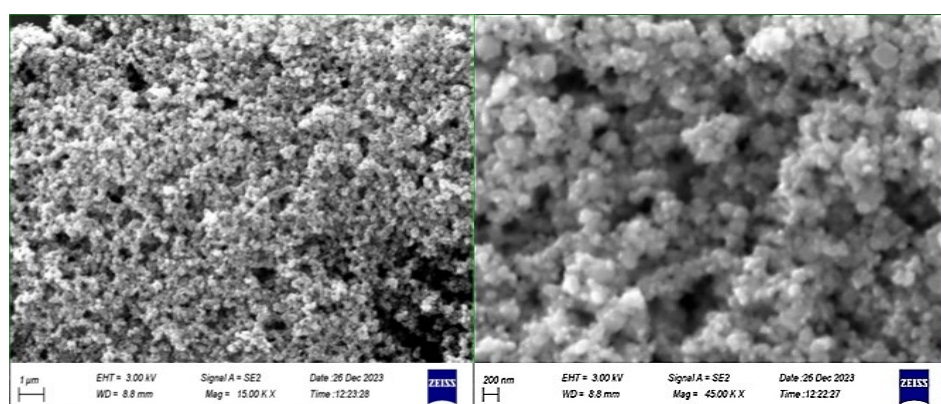


**Figure 6.** SEM images of silver nanoparticles synthesized using *Cymbopogon citratus* leaf extract, showing spherical morphology and size distribution.

### 3.2. Antibacterial activity of silver nanoparticles

Figure 7 shows zones of inhibition against eight test organisms as antibacterial activity of silver nanoparticles (AgNPs). Table 1 summarizes the inhibition zones, which clearly indicate that AgNPs have shown high inhibitory effects on *Proteus mirabilis*, *Bacillus subtilis*, *Staphylococcus aureus*, *Escherichia coli*, *Klebsiella pneumoniae*, *Vibrio cholerae*, *Vibrio parahaemolyticus* and *Salmonella enteritidis* with average diameters of 30.33 mm, 24.67 mm, 30 mm, 25.33 mm, 28.67 mm, 32.67 mm, 34.67 mm and 30.67 mm inhibition zones respectively.

**Table 1.** Antibacterial activity of silver nanoparticles against eight bacterial strains, expressed as the average diameter of inhibition zones (mm).

Bacterial isolate	Inhibition zone rate (mm)
<i>Proteus mirabilis</i>	30.33
<i>Bacillus subtilis</i>	24.67
<i>Staphylococcus aureus</i>	30
<i>Escherichia coli</i>	25.33
<i>Klebsiella pneumonia</i>	28.67
<i>Vibrio parahaemolyticus</i>	32.67
<i>Vibrio parahaemolyticus</i>	34.67
<i>Salmonella enteritidis</i>	30.67

The antibacterial mechanism of silver nanoparticles is by attachment to the membrane of bacterial cell thus disrupting key functions of the cell membrane such as permeability and respiration. AgNPs can penetrate inside the bacterial as well as the fungal cells and also leave an impact on spore membrane integrity which results in total cell death. Silver nanoparticles interact with sulfur containing proteins as well as DNA phosphorus containing residues in the microbial cells<sup>[28,29]</sup>. Our results indicate high efficiency against both Gram-positive and Gram-negative bacteria, consistent with recent findings in the literature<sup>[28,29]</sup>. The maximum inhibition zone of 34.67 mm against *Vibrio parahaemolyticus* suggests particularly high sensitivity of this strain to the biosynthesized AgNPs compared to other tested strains.



**Figure 7.** Photographic images of Petri dishes showing the antibacterial effects of silver nanoparticles on *Proteus mirabilis*, *Bacillus subtilis*, *Staphylococcus aureus*, *Escherichia coli*, *Klebsiella pneumoniae*, *Vibrio cholerae*, *Vibrio parahaemolyticus*, and *Salmonella enteritidis*.

## 4. Conclusion

Silver nanoparticles were synthesized by green chemistry using the extract from leaves of *Cymbopogon citratus*. This method proves to be friendly to the environment, low-cost, and non-toxic. XRD analysis confirmed single-phase crystalline formation in AgNPs. SEM, AFM together with DLS studies revealed that synthesized particles are within nanometer size range. Further study on antimicrobial activities indicated strong effects against eight strains of bacteria which include *Proteus mirabilis*, *Bacillus subtilis*, *Staphylococcus aureus*, *Escherichia coli*, *Klebsiella pneumoniae*, *Vibrio cholerae*, *Vibrio parahaemolyticus* and *Salmonella enteritidis* with inhibition zone diameters ranging between 24.67-34.67 mm specifically 30.33, 24.67, 30, 25.33, 28.67, 32.67, 34.67, and 30.67 mm, respectively. This study successfully demonstrates the potential of *C. citratus* extract as an effective reducing and capping agent for stable, spherical AgNPs. A key finding is the potent antibacterial effect against the pathogenic *Vibrio parahaemolyticus*. Limitations of this study include the need for further optimization of synthesis parameters and a deeper investigation into the specific phytochemical mechanisms responsible for the reduction process. Future research should focus on exploring the application of these CC-Ag NPs in biomedical fields, such as targeted drug delivery systems, antifungal treatments, and potential antiviral properties, using established clinical protocols.

## Conflict of interest

The authors declare no conflict of interest.

## References

1. Bawa, R., Audette, G.F. and Rubinstein, I. (2016) Handbook of clinical nanomedicine: nanoparticles, imaging, therapy, and clinical applications. Pan Stanford.
2. Kushwaha, A.; Singh, V.K.; Bhartariya, J.; Singh, P. and Yasmeen, K. (2015). Isolation and identification of *E. coli* bacteria for the synthesis of silver nanoparticles: characterization of the particles and study of antibacterial activity. *Eur J Exp Biol.* 5: 65-70.
3. Luceri, A., Francese, R., Lembo, D., Ferraris, M., & Balagna, C. (2023). Silver nanoparticles: review of antiviral properties, mechanism of action and applications. *Microorganisms*, 11(3), 629.
4. Mittal, A.K., Chisti, Y. and Banerjee, U.C. (2013). Synthesis of metallic nanoparticles using plant extracts. *Biotechnology advances*. 31(2): 346-356.
5. Rahimi-Nasrabadi, M., Pourmortazavi, S.M., Shandiz, S.A.S., Ahmadi, F. and Batooli, H. (2014). Green synthesis of silver nanoparticles using *Eucalyptus leucoxylon* leaves extract and evaluating the antioxidant activities of extract. *Natural product research*. 28(22):1964-1969.
6. Pirayei, M., Abolghasemi, M.M. and Nazemiyeh, H. (2015). Fast determination of *Ziziphora tenuior* L. essential oil by inorganic-organic hybrid material based on ZnO nanoparticles anchored to a composite made from polythiophene and hexagonally ordered silica. *Natural product research*. 29(9): 833-837.
7. Lekha, D. C., Shanmugam, R., Madhuri, K., Dwarampudi, L. P., Bhaskaran, M., Kongara, D., & Krishnaraj, R. (2021). Review on silver nanoparticle synthesis method, antibacterial activity, drug delivery vehicles, and toxicity pathways: recent advances and future aspects. *Journal of Nanomaterials*, 2021(1), 4401829.
8. Sathishkumar, M., Sneha, K. and Yun, Y.S. (2010). Immobilization of silver nanoparticles synthesized using *Curcuma longa* tuber powder and extract on cotton cloth for bactericidal activity. *Bioresour. Technol.* 101(20):7958-7965.
9. Suganya, A.; Murugan, K.; Kovendan, K.; Mahesh Kumar, P. and Hwang, JS. (2013) Green synthesis of silver nanoparticles using *Murraya koenigii* leaf extract against *Anopheles stephensi* and *Aedes aegypti*. *Parasitol Res.* 112:1385-1397.
10. Murugan, K.; Benelli G.; Suganya, A.; Dinesh, D.; Panneerselvam, C.; Nicoletti, M.; Hwang, JS; Mahesh; Kumar, P.; Subramaniam, J. and Suresh, U. (2015). Toxicity of seaweed-synthesized silver nanoparticles against the filariasis vector *Culex quinquefasciatus* and its impact on predation efficiency of the cyclopoid crustacean *Mesocyclops longisetus*. *Parasitol Res.* 14:2243-2253.
11. Madhiyazhagan, P.; Murugan, K.; Kumar, A.N.; Nataraj, T.; Dinesh, D.; Panneerselvam, C.; Subramaniam, J.; Kumar, P.M.; Suresh, U.; Roni, M. and Nicoletti, M. (2015). Sargassum muticum-synthesized silver nanoparticles: an effective control tool against mosquito vectors and bacterial pathogens. *Parasitology research*. 114(11): 4305-4317.

12. Aibinu, I., Adenipekun, T., Adelowotan, T., Ogunsanya, T. and Odugbemi, T. (2007). Evaluation of the antimicrobial properties of different parts of *Citrus aurantifolia* (lime fruit) as used locally. *African Journal of Traditional, Complementary, and Alternative Medicines*. 4(2): 185.
13. Shah, G., Shri, R., Panchal, V., Sharma, N., Singh, B. and Mann, A.S., (2011). Scientific basis for the therapeutic use of *Cymbopogon citratus*, staph (Lemon grass). *Journal of advanced pharmaceutical technology and research*. 2(1):3.
14. Abegaz, B., Yohannes, P.G. and Dieter, R.K. (1983). Constituents of the essential oil of Ethiopian *Cymbopogon citratus* Staph. *Journal of Natural products*. 46(3): 424-426.
15. Negrelle, R.R.B. and Gomes, E.C. (2007). *Cymbopogon citratus* (DC.) Staph: chemical composition and biological activities. *Rev Bras Pl Med*. 9(1): 80-92.
16. Alharbi, N. S., Alsubhi, N. S., & Felimban, A. I. (2022). Green synthesis of silver nanoparticles using medicinal plants: Characterization and application. *Journal of Radiation Research and Applied Sciences*, 15(3), 109-124.
17. Fadeel, B. (2014) *Handbook of safety assessment of nanomaterials: From toxicological testing to personalized medicine*. Pan Stanford.
18. Anbukkarasi, M., Thomas, P.A., Sheu, J.R. and Geraldine, P. (2017). In vitro antioxidant and anticataractogenic potential of silver nanoparticles biosynthesized using an ethanolic extract of *Tabernaemontana divaricata* leaves. *Biomedicine and Pharmacotherapy*. 91: 467-475.
19. Jena, S.; Singh, R.K.; Panigrahi, B.; Suar, M. and Mandal, D. (2016). Photo-bioreduction of Ag<sup>+</sup> ions towards the generation of multifunctional silver nanoparticles: Mechanistic perspective and therapeutic potential. *Journal of Photochemistry and Photobiology B: Biology*. 164: 306-313.
20. Gopinath, V.; MubarakAli, D.; Priyadarshini, S.; Priyadharshini, N.M.; Thajuddin, N. and Velusamy, P. (2012). Biosynthesis of silver nanoparticles from *Tribulus terrestris* and its antimicrobial activity: a novel biological approach. *Colloids and Surfaces B: Biointerfaces*. 96:69-74.
21. Nath, S. S., Chakdar, D., Gope, G., & Avasthi, D. K. (2008). Effect of 100 MeV nickel ions on silica coated ZnS quantum dots. *Journal of Nanoelectronics and Optoelectronics*, 3(2), 180-183.
22. K.P. Bankura, D. Maity, M.M.R. Mollick, D. Mondal, B. Bhowmick, M.K. Bain, A. Chakraborty, J. Sarkar, K. Acharya, and D. Chattopadhyay, Synthesis, characterization and antimicrobial activity of dextran stabilized silver nanoparticles in aqueous medium, *Carbohydr. Polym.*, 89(2012), No. 4, p. 1159.
23. Erjaee, H., Rajaian, H., & Nazifi, S. (2017). Synthesis and characterization of novel silver nanoparticles using Chamaemelum nobile extract for antibacterial application. *Advances in Natural Sciences: Nanoscience and Nanotechnology*, 8(2), 025004.
24. Mittal, J., Jain, R., & Sharma, M. M. (2017). Phytofabrication of silver nanoparticles using aqueous leaf extract of *Xanthium strumerium* L. and their bactericidal efficacy. *Advances in Natural Sciences: Nanoscience and Nanotechnology*, 8(2), 025011.
25. Ahmad, N., Bhatnagar, S., Ali, S. S., & Dutta, R. (2015). Phytofabrication of bioinduced silver nanoparticles for biomedical applications. *International journal of nanomedicine*, 10, 7019.
26. Venil, C. K., Sathishkumar, P., Malathi, M., Usha, R., Jayakumar, R., Yusoff, A. R. M., & Ahmad, W. A. (2016). Synthesis of flexirubin-mediated silver nanoparticles using *Chryseobacterium artocarpi* CECT 8497 and investigation of its anticancer activity. *Materials Science and Engineering: C*, 59, 228-234.
27. Huang, J., Li, Q., Sun, D., Lu, Y., Su, Y., Yang, X., ... & Hong, J. (2007). Biosynthesis of silver and gold nanoparticles by novel sundried *Cinnamomum camphora* leaf. *Nanotechnology*, 18(10), 105104.
28. Shaaban, M. T., Mohamed, B. S., Zayed, M., & El-Sabbagh, S. M. (2024). Antibacterial, antibiofilm, and anticancer activity of silver-nanoparticles synthesized from the cell-filtrate of *Streptomyces enissocaeulis*. *BMC biotechnology*, 24(1), 8.
29. Suresh, U.; Murugan, K.; Benelli, G.; Nicoletti, M.; Barnard, DR.; Panneerselvam, C.; Mahesh Kumar, P.; Subramaniam, J.; Dinesh, D. and Chandramohan, B. (2015) Tackling the growing threat of dengue: *Phyllanthus niruri*-mediated synthesis of silver nanoparticles and their mosquitocidal properties against the dengue vector *Aedes aegypti* (Diptera: Culicidae). *Parasitol Res*. 114:1551–1562.